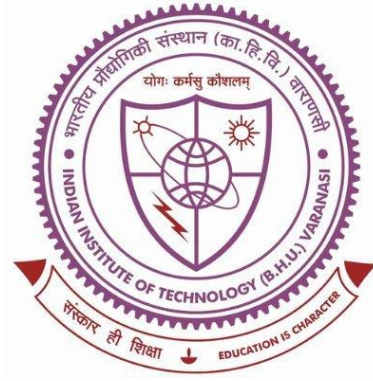


Numerical and experimental studies on single phase natural circulation loop using water and oil based hybrid nanofluids



Thesis submitted in partial fulfillment for the
Award of Degree

Doctor of Philosophy

By

Mayaram Sahu

DEPARTMENT OF MECHANICAL ENGINEERING
INDIAN INSTITUTE OF TECHNOLOGY
(BANARAS HINDU UNIVERSITY)
VARANASI-221005
INDIA

Roll No. 17131012

2022

CERTIFICATE

It is certified that the work contained in the thesis titled “**Numerical and experimental studies on single phase natural circulation loop using water and oil based hybrid nanofluids**” by Mayaram Sahu has been carried out under our supervision and that this work is not submitted elsewhere for any degree.

It is further certified that the student has satisfactorily fulfilled all the requirements of the Comprehensive examination, Candidacy, and SOTA for the award of the Ph.D. degree.



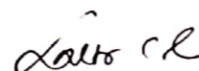
29.7.22

Prof. Jahar Sarkar

(Supervisor)

Department of Mechanical Engineering

IIT (BHU) Varanasi



Dr. Laltu Chandra

(Co-supervisor)

Department of Mechanical Engineering


IIT (BHU) Varanasi

DECLARATION BY THE CANDIDATE

I, **Mayaram Sahu**, certify that the work embodied in this thesis is my own bonafide work carried out by me under the supervision of **Prof. Jahar Sarkar** and **Dr. Laltu Chandra** for a period of 5 years from July 2017 to July 2022 at IIT (BHU), Varanasi. The material contained in this thesis has not been submitted for the award of any other degree. I declare that I have faithfully acknowledged and given credits to the research workers wherever their works have been cited in my work in this thesis. I further declare that I have not willfully copied any others' work, paragraphs, text, data, results, etc. reported in journals, books, magazines, reports, dissertations, theses, etc. or available at websites and have not included them in this thesis and have not cited as my own work.

Date: 29/07/22

Place: IIT (BHU), Varanasi


(Mayaram Sahu)

CERTIFICATE BY THE SUPERVISORS

This is to certify that the above statement made by the candidate is correct to the best of my knowledge.


29.7.22

Prof. Jahar Sarkar

(Supervisor)



Dr. Laltu Chandra

(Co-supervisor)


Head of the Department

Mechanical Engineering Department, IIT (BHU), Varanasi

विभागाध्यक्ष / HEAD

यान्त्रिक अभियान्त्रिकी विभाग / Deptt. of Mechanical Engg.

भारतीय प्रौद्योगिकी संस्थान / Indian Institute of Technology

(का ii U.)

संस्थान संख्या / Institute Number: 221005

COPYRIGHT TRANSFER CERTIFICATE

Title of the Thesis: **Numerical and experimental studies on single phase natural circulation loop using water and oil based hybrid nanofluid.**

Candidate's Name: **Mayaram Sahu**

COPYRIGHT TRANSFER

The undersigned hereby assigns to the Indian Institute of Technology (Banaras Hindu University) Varanasi all rights under copyright that may exist in and for the above thesis submitted for the award of the Ph.D. degree.

Date: 29/07/2022

Place: IIT (BHU), Varanasi

A handwritten signature in blue ink that reads "M. P. Sahu." with a long horizontal stroke extending to the right.

(Mayaram Sahu)

Note: However, the author may reproduce or authorize others to reproduce material extracted verbatim from the thesis or derivative of the thesis for author's personal use provided that the source and University's copyright notice are indicated.

ACKNOWLEDGEMENTS

I take this opportunity to express my deep sense of gratitude to my supervisor **Prof. Jahar Sarkar** and **Dr. Laltu Chandra** for their continuous guidance and whole-hearted cooperation in carrying out this work. His meticulous and valuable review and constructive criticism of the manuscript have greatly improved the quality of work. Sir, for your faith in me and the desire to live up to your expectations, has constantly pushed me to work harder.

My grateful appreciation also goes to **Prof. Pradyumna Ghosh** and **Dr. Ravi P. Jaiswal** for serving on my research progress evaluation committee (RPEC). Thank you all for sparing your valuable time and assisting me throughout my research and completion of this thesis. I wish to extend my sincere thanks to **Prof. Santosh Kumar**, Head, Department of Mechanical Engineering for providing me the necessary resources to enable me to complete this research work. During my stay at IIT (BHU) Varanasi, I have met many people who have made this period of my life memorable and very pleasant. Among them, I would like to sincerely acknowledge the assistance and motivation provided by **Dr. Rashmi Rekha Sahoo, Dr. Swasti Sundar Mandal, Dr. Om Prakash Singh and Dr. Amitesh kumar**. I want to thank my colleagues at IIT (BHU) Varanasi, especially to **Mr. Prashant Srivastava, Mr. Satish Upadhyay, Mrs. Archana Kumari, Mr. Mayank Srivastava, Mr. Jayprakash, and Mr. Sarvesh Kashyap** for encouraging me to finish this work. The experimental part of this thesis has been carried out at the Department of Mechanical Engineering IIT (BHU) Varanasi. A number of persons have assisted and supported me in designing and development of the test rig. I would like to extend my sincere thanks to **Mr. Mulchand** and **Mr. Sunil bardhan** for giving the valuable ideas while performing experiments and providing the measurement tools and instruments whenever needed for the research work without any hesitation.

I would like to acknowledge my parents, especially my elder brother (**Heturam Sahu**) and family for not engaging me in any other affairs during my research duration and handling all the matters by themselves. I thank my parents for assisting me financially whenever needed and motivating me for

my work. Your sacrifices for allowing me to completely devote my attention to my research work are greatly acknowledged and appreciated.

I would also like to thank GOD the Almighty for giving me the strength to remain on the path to success.

Date: 29/07/2022

Place: IIT (BHU), Varanasi

A handwritten signature in blue ink, reading "M. P. Sahu." with a horizontal line drawn through the text.

(Mayaram Sahu)

TABLE OF CONTENTS

Chapter 1: Introduction	1
1.1 Background and motivation	1
1.2 Natural circulation loop	3
1.3 Mono and hybrid nanofluids	6
1.4 Objective and novelty of the thesis.....	8
1.5 Thesis structure.....	10
Chapter 2: Literature review.....	12
2.1 Experimental Studies	12
2.2 Theoretical and numerical studies	19
2.3 Research gaps.....	24
Chapter 3: Numerical modelling for Single Phase Natural Circulation Loop using various working fluids.....	27
3.1 Methodology.....	27
3.1.1 Governing Equations	28
3.1.2 Properties of the working fluids	30
3.1.3 Nusselt number and friction factor	32
3.1.4 Numerical scheme and performance parameters	34
3.1.5 Grid and time-independent test.....	36
3.1.6 Model validation.....	39

3.2	Results and discussion	40
3.2.1	Water-based binary hybrid nanofluids.....	40
3.2.2	Water-based ternary hybrid nanofluids	59
3.2.3	Thermal oils.....	71
3.3	Important findings	77

Chapter 4: Effect of modelling assumptions on SPNCL performances 79

4.1	Methodology	79
4.1.1	Governing Equations:.....	81
4.1.2	Properties of working fluids.....	84
4.1.3	Nusselt number and friction factor correlation	85
4.1.4	Numerical scheme and performance parameters	87
4.1.5	Grid and time-independent test.....	88
4.2	Results and Discussion	88
4.2.1	Effect of various assumptions on the performance of VHHC SPNCL .	89
4.2.2	Effect of different working fluids on the performance of VHHC SPNCL	97
4.2.3	Influence of different nature of heat flux distribution on the performance parameters.....	104
4.3	Important highlights	111

Chapter 5: Experimentation on SPNCL using water-based mono/hybrid nanofluids	113
5.1 Preparation of and Characterization.....	113
5.1.1 Preparation of mono/hybrid nanofluids	113
5.1.2 Characterization of nanoparticles	115
5.1.3 Stability of mono/hybrid nanofluids	116
5.1.4 Calculation of thermophysical properties of nanofluids	117
5.2 Experimentation methodology	118
5.2.1 Experimental setup and instrumentation	118
5.2.2 Experimental procedure.....	122
5.2.3 Data analysis and performance parameter	123
5.2.4 Uncertainty analysis.....	124
5.3 Results and discussion.....	125
5.3.1 Repeatability test.....	126
5.3.2 Comparison of the experimental and numerical results	126
5.3.3 Transient behavior of SPNCL for various hybrid nanofluids.....	127
5.3.4 Influence of input power on steady-state performance parameter	130
5.3.5 Effect of coolant inlet temperature on the performance parameters..	133
5.3.6 Effect of loop inclination on the performance parameter	136
5.4 Important findings.....	140

Chapter 6: Experimental investigations of SPNCL using mono/hybrid nano-oils 142

6.1 Experimentation methodology 142

6.1.1 Experimental setup and procedure142

6.1.2 Nano-oil preparation, characterization and properties143

6.1.3 Evaluation of performance parameters145

6.1.4 Uncertainty analysis.....147

6.2 Results and discussion 147

6.2.1 Repeatability test.....148

6.2.2 Comparison of experimental and numerical results.....149

6.2.3 Transient behavior of SPNCL for mono/hybrid nano-oils150

6.2.4 Effect of input power on the transient and steady-state performance parameters.....152

6.2.5 Effect of loop inclination on the performance parameters160

6.2.6 Performance comparison of Therminol VP1 and Soyabean oil168

6.3 Important findings..... 170

Chapter 7: Conclusions and future scope 171

7.1 Conclusions 171

7.2 Future scope 173

References.....175-189

List of Publications.....190-191

TABLE OF FIGURES

Fig. 1.1. Fuel share of CO ₂ emissions from fuel combustion, 1973 and 2019 (IEA, CO ₂ Emissions from Fuel Combustion, 2021) [1].....	2
Fig. 1.2: Share of world total energy supply by source, 1973 and 2019 (IEA, World Energy Balances, 2021) [1]	2
Fig. 1.3 Schematic diagram of rectangular Single phase natural circulation loop	4
Fig. 1.4: Application of natural circulation loop.....	5
Fig. 3.1 Schematic of SPNCL with Vertical Heater Vertical Cooler arrangement	28
Fig. 3.2 A schematic of an inclined SPNCL	29
Fig. 3.3 Temporal variation of mass flow rate for (a) different grid sizes and the time-step $\Delta t = 0.1$ s and (b) different time steps and the grid size of 0.03 m.	38
Fig. 3.4 (a) Comparison of numerical mass flow rate with experimental at the steady-state. (b) Comparison of transient pressure drop with experimental result by Vijayan et al. [97].	40
Fig. 3.5 Variation of primary fluid (a) temperature along the loop at various instants of time (b) Temporal mass flow rate.	43
Fig. 3.6 Temporal variation of a mass flow rate of water-based binary hybrid nanofluids at 500 W and 301 K sink temperature.	45
Fig. 3.7 Influence of heater power on temporal mass flow rate for Al ₂ O ₃ +Ag hybrid nanofluid.	46
Fig. 3.8 Influence of loop diameter on the temporal variation of mass flow rate for Al ₂ O ₃ +Ag hybrid nanofluid.	47
Fig. 3.9 Influence of loop height on the temporal variation of mass flow rate for Al ₂ O ₃ +Ag hybrid nanofluid.....	48

Fig. 3.10 Effect of heater power input on mass flow rate for different binary hybrid nanofluids.....	49
Fig. 3.11 Effect of power input on the effectiveness for different binary hybrid nanofluids	51
Fig. 3.12 Effect of power input on the total entropy generation for different binary hybrid nanofluids.....	51
Fig. 3.13 Effect of diameter on steady state mass flow rate for Al ₂ O ₃ + Ag+ Water hybrid nanofluids.....	53
Fig. 3.14 Effect of diameter on the effectiveness for Al ₂ O ₃ + Ag+ Water hybrid nanofluids	53
Fig. 3.15 Effect of diameter on the total entropy generation for Al ₂ O ₃ + Ag+ Water hybrid	53
Fig. 3.16 Effect of loop height on steady state mass flow rate for Al ₂ O ₃ + Ag+ Water.....	55
Fig. 3.17 Effect of loop height on the effectiveness for Al ₂ O ₃ + Ag+ Water.....	55
Fig. 3.18 Effect of loop height on the total entropy generation for Al ₂ O ₃ + Ag+ Water....	56
Fig. 3.19 Effect of loop inclination on the steady state mass flow rate for Al ₂ O ₃ + Ag+ Water.....	57
Fig. 3.20 Effect of loop inclination on the effectiveness for Al ₂ O ₃ + Ag+ Water.....	58
Fig. 3.21 Effect of loop inclination on the total entropy generation rate for Al ₂ O ₃ + Ag+ Water.....	58
Fig. 3.22 Transient variation of mass flow rate for different water based ternary hybrid nanofluids at 500 W input power.....	61
Fig.3.23 The fluid temperature distribution along the loop for water and Al ₂ O ₃ +Cu+CNT+water at 500 W power input.....	62
Fig. 3.24 Variation of computed steady-state mass flow rate with input power.	63

Fig. 3.25 Computed steady-state effectiveness at various input power.	64
Fig. 3.26 The computed steady-state entropy generation rate various input power.	65
Fig. 3.27 The computed steady-state mass flow rate at various inclinations of loop.	69
Fig. 3.28 The computed steady-state effectiveness at a various loop inclination angle	69
Fig. 3.29 The computed steady-state total entropy generation rate at various loop inclination angle.	70
Fig. 3.30 Comparison of transient variation of mass flow rate with water and thermal oils	72
Fig. 3.31 Steady-state mass flow rate for water and thermal oils.	73
Fig. 3.32 Effectiveness of heat exchanger for water and thermal oils	73
Fig. 3.33 Total entropy generation rate for water and thermal oils.	74
Fig. 3.34 Variation of steady-state mass flow rate with height-to-width ratio for thermal oils.	75
Fig. 3.35 Variation of effectiveness with height-to-width ratio for thermal oils.	76
Fig. 3.36 Variation of entropy generation rate with height-to-width ratio for thermal oils.	77
Fig. 4.1 Schematic illustration of VHHC Single phase natural circulation loop, (b) Cross sectional view of heating section and (c) Cross sectional view of cooler section	81
Fig. 4.2 Comparison of steady state mass flow rate obtained numerically for different cases (i-vi) with experimental data [97] using water.	91
Fig. 4.3 Effect of different cases (i-vi) on steady state effectiveness of cooler with power input.	92
Fig. 4.4 Effect of different cases (i-vi) on steady-state total entropy generation rate with power input.	93

Fig. 4.5 Comparison of transient pressure drop obtained by different cases (i-vi) with experimental data [97] using water.....	95
Fig. 4.6 Effect of different cases (i-vi) on the transient mass flow rate.....	96
Fig. 4.7 Effect of different base fluids on deviation in mass flow rate with power input .	98
Fig. 4.8 Show the constant and variable thermophysical properties variation with temperature, (a) Density, (b) Specific heat, (c) thermal conductivity, and (d) Viscosity of the different base fluids respectively.	100
Fig. 4.9 Effect of different working fluids on deviation in effectiveness with power input.	101
Fig. 4.10 Deviation in entropy generation with power input for different working fluids	102
Fig. 4.11 Comparison of transient mass flow rate of case (i) and case (vi) for different working fluids.	104
Fig. 4.12 Different heat flux distribution nature along the heating length	105
Fig. 4.13 Effect of different heat flux distribution nature on transient mass flow rate for Al ₂ O ₃ +Cu +Water	106
Fig. 4.14 Effect of different heat flux distribution nature on steady mass flow rate for Al ₂ O ₃ +Cu +Water.	107
Fig. 4.15 Effect of different heat flux distribution nature on effectiveness for Al ₂ O ₃ +Cu +Water.	108
Fig. 4.16 Temperature distribution along loop length for different heat flux distribution nature for Al ₂ O ₃ +Cu +Water.	109
Fig. 4.17 Effect of different heat flux distribution nature on total entropy generation for Al ₂ O ₃ +Cu +Water.	110

Fig. 5.1 Flow chart of preparation of mono/hybrid nanofluids, nanoparticles, and equipment used for the preparation of nanofluids	114
Fig. 5.2 SEM image (a) Al_2O_3 particle (b) Al_2O_3 +CNT nanoparticles mixture	116
Fig. 5.3 Photographs of prepared nano/hybrid nanofluids with time	117
Fig. 5.4 (a) Schematic layout out Experimental facility, (b) Photographic view of Experimental facility.....	120
Fig. 5.5 The measured water mass flow rate for three different experiments under an identical operating condition to ensure repeatability.....	126
Fig. 5.6 Comparison of experimental transient mass flow rate with the numerical result for different power inputs	127
Fig. 5.7 Experimental transient mass flow rate for different mono/hybrid nanofluids....	129
Fig. 5.8 Experimental transient heater temperature difference for different Fluids.	129
Fig. 5.9 Steady-state mass flow rate for different mono/hybrid nanofluids at power input.	131
Fig. 5.10 Steady state effectiveness for different water-based mono/hybrid nanofluid at different power input.....	131
Fig. 5.11 Steady state total entropy generation rate for different mono/hybrid nanofluids at different power input.....	132
Fig. 5.12 Experimental transient mass flow rate at different coolant inlet temperatures	133
Fig. 5.13 Steady state experimental mass flow rate for different water-based mono/hybrid nanofluids at different coolant inlet temperatures	134
Fig. 5.14 Steady state experimental effectiveness for different water-based mono/hybrid nanofluids at different coolant inlet temperatures	135
Fig. 5.15 Steady state experimental total entropy generation rate for different water-based mono/hybrid nanofluids at different coolant inlet temperatures.....	135

Fig. 5.16 a) Counter clockwise inclination of the loop, (b) Clock wise inclination of the loop from vertical.....	136
Fig. 5.17 Experimental transient mass flow rate for different loop inclinations	137
Fig. 5.18 Variation of the central distance between heater and cooler at different loop inclination	138
Fig. 5.19 Steady state experimental mass flow rate for different water-based mono/hybrid nanofluids at different loop inclinations	138
Fig. 5.20 Steady state experimental effectiveness for different water-based mono/hybrid nanofluids at different loop inclinations	139
Fig. 5.21 Steady state experimental effectiveness for different water-based mono/hybrid nanofluids at different loop inclinations	139
Fig. 6.1 Photographic view of the installed single-phase natural circulation loop (SPNCL) experimental facility.	143
Fig. 6.2 Variation of thermophysical properties: (a) density, (b) specific heat capacity, (c) thermal conductivity, and (d) absolute viscosity for the primary fluids	145
Fig. 6.3 The measured temperature with Soyabean oil at the inlet and outlet of heater for three different experiments and at an identical operating condition for repeatability.	149
Fig. 6.4 A comparison between the experimental and numerical temperature difference across the heater for an input power of 400 W at the transient and steady-state conditions.	150
Fig. 6.5 Experimental temperature difference across the heater for the TVP1-based mono and hybrid nano-oils.	151
Fig. 6.6 Experimentally obtained temperature difference across the heater for the Soyabean oil-based mono and hybrid nano-oils.....	151

Fig. 6.7 Experimentally obtained temperature difference across the heater for TVP1 at different input powers	153
Fig. 6.8 Experimentally obtained temperature difference across the heater for Soyabean oil at different input powers.	153
Fig. 6.9 Temperature distribution along loop length at different power input for (a) Therminol VP1 and (b) soyabean oil.	154
Fig. 6.10 Steady state mass flow rate for different Therminol VP1-based mono/hybrid nanofluids with power input.	156
Fig. 6.11 Steady state mass flow rate for different soyabean-based mono/hybrid nanofluids with power input.	157
Fig. 6.12 Steady-state effectiveness of cooler for TVP1 based nano-oils for the different input powers.....	158
Fig. 6.13 Steady-state effectiveness of cooler for Soyabean oil and its nano-oils for the different input powers.	158
Fig. 6.14 The total entropy generation rates at the steady-state conditions for TVP1 and TVP1-based nano-oils at different input powers	159
Fig. 6.15 The total entropy generation rates at the steady-state conditions for Soyabean oil and Soyabean oil-based nano-oils at different input powers.	160
Fig. 6.16 The photographs showing VHHC arrangement of SPNCL with (a) counter-clockwise and (b) clockwise inclinations	161
Fig. 6.17 Experimental transient temperature differences across the heater for the different loop inclinations with TVP1	162
Fig. 6.18 Experimental transient temperature differences across the heater for the different loop inclinations with Soyabean oil.....	162

Fig. 6.19 Variation of the central distance between heater and heat exchanger at different loop inclinations.....	163
Fig. 6.20 Steady state experimental mass flow rate for different Therminol VP1-based mono/hybrid nanofluids at different loop inclinations.....	163
Fig. 6.21 Steady-state experimental mass flow rate for different Soyabean-based mono/hybrid nanofluids at different loop inclinations.....	164
Fig. 6.22 Steady state experimental effectiveness for different Therminol VP1-based mono/hybrid nanofluids at different loop inclination	165
Fig. 6.23 Steady state experimental effectiveness for different Soyabean-based mono/hybrid nanofluids at different loop inclination	165
Fig. 6.24 Steady state experimental total entropy generation rate for different Therminol VP1-based mono/hybrid nanofluids at different loop inclination.....	167
Fig. 6.25 Steady state experimental total entropy generation rate for different soyabean-based mono/hybrid nanofluids at different loop inclination	167
Fig. 6.26 Performance assessment of VHHC configuration of SPNCL with TVP1 with Soyabean oil based on (a) mass flow rate (b) effectiveness and (c) total entropy generation rate.....	169

LIST OF TABLES

Table 1.1 Temperature range, application and working fluid of SPNCL	5
Table 2.1 Some important experimental investigations on SPNCL	17
Table 2.2 Some important numerical investigations on SPNCL	22
Table 3.1 Some important numerical investigations on SPNCL [99-104].	31
Table 3.2 Sphericity, Empirical shape factor, and viscosity enhancement coefficient of different shapes of nanoparticles [105].	32
Table 3.3 Calculation of discretization error.	36
Table 3.4 Operating condition and geometric parameter used in this analysis.	41
Table 3.5 Geometric parameter and operating condition considered in the analysis.	59
Table 3.6 The performance enhancement of SPNCL using binary and ternary water-based nanofluid compared to water at 100 W.	66
Table 3.7 Geometric parameter and operating condition considered in this analysis.	71
Table 4.1 Thermophysical properties of nanoparticles [99].	85
Table 4.2 Considered geometric and operating parameters of VHHC SPNCL.	88
Table 4.3 The effect of different cases (ii-vi) on the performance parameter compared to case(i) at 1000 W power input.	96
Table 4.4 Buoyancy force calculation for different nature of heat flux distribution.	107
Table 5.1 Particle size, shape, and thermophysical properties of nanoparticles used in the investigation [118]	115
Table 5.2 Position of the thermocouples.	120
Table 5.3 Geometric parameters and materials used in the experimentation.	121
Table 5.4 Instruments and their specification used to measure the different parameters	121
Table 5.5 Maximum uncertainties of the calculated parameters	124
Table 5.6 Operating parameters of VHHC SPNCL.	125

Table 6.1 Maximum uncertainties of the calculated parameters for the TVP1.	147
Table 6.2 Maximum uncertainties of the calculated parameters for the Soyabean oil. ...	147
Table 6.3 Operating parameters for VHHC configuration of SPNCL.....	148

LIST OF THE SYMBOLS

NOMENCLATURE

A	Cross section area (m ²)
c_p	Specific heat (J/kg-K)
d	Loop tube diameter (m)
f	Friction factor
g	Acceleration due to gravity, m/s ²
h	Coefficient of heat transfer (W/m ² -K)
k	Thermal conductivity, W/m-K
K	Local loss coefficient
L _C	Cooler length (m)
L _H	Heater length (m)
L _t	Total length of the loop (m)
m	Empirical shape factor
\dot{m}	Mass flow rate (kg/s)
Q	Input power (W)
Ra	Rayleigh number
s	Axial space coordinate (m)
S _{gen}	Entropy generation rate (W/K)
t	Time (s)
T	Fluid temperature (K)
w	Tube wall
V	Volume, m ³

Greek Symbols

α	Thermal diffusivity (m^2/s)
β	Volumetric expansion coefficient, ($1/\text{K}$)
μ	Dynamic viscosity of fluid ($\text{N}\cdot\text{s}/\text{m}^2$)
θ	Change in direction of flow (deg)
φ	Angle of loop inclination (deg)
ϕ	Volume fraction of nanoparticle
ρ	Fluid density (kg/m^3)
ε	Effectiveness
ξ	Perimeter, m

Subscripts

0	References point
avg	Average
1,2,3	Nanoparticle types
c,h	hot leg, cold leg
C,H	Cooler, Heater
bf	Base fluid
hnf	hybrid nanofluid
in	inlet
ins	insulation
out	outlet
p	Nanoparticle
S	secondary fluid
t	total
W	tube wall

Abbreviations

EG	Ethylene Glycol
HF	Heat Flux
PG	Propylene Glycol
SPNCL	Single-Phase Natural Circulation Loop
TR	Temperature ratio
VHHC	Vertical heating horizontal cooling
HHHC	Horizontal heating horizontal cooling
TVP1	Therminol VP1

ABSTRACT

Global urbanization and industrialization processes are causing a significant rise in energy usage. The growing energy demand requires a reliable passive device like a natural circulation loop for heat recovery, transfer and use. The selection of a single-phase natural circulation loop is motivated by the independence of any mechanical device or active power source for its simple operation. The difference between buoyancy, generated by the heating and cooling, and pressure-drop leads to the setting up of flow in a natural circulation loop. The safety, reliability, and maintenance cost motivate the use of natural circulation loops for power generation, viz. solar thermal and nuclear, heating and cooling applications, etc., in industries. The literature review revealed the dearth and potential for hybrid nanofluids that are envisaged as a promising working fluid in the futuristic natural circulation loops. Furthermore, many related issues have to be explored, such as the effect of nanoparticle shape and using hybrid nanofluids, the effect of various assumptions for numerical modelling and the effect of oil and nano-oil for medium temperature applications. Considering these issues, the present thesis includes detailed numerical and experimental investigations of a single-phase natural circulation loop with the vertical heater and the vertical cooler arrangement. The objectives are to evaluate the transient and steady-state thermo-hydraulic behaviour, energetic and exergetic performances using water-based binary and ternary hybrid nanofluids for low temperature ($< 100\text{ }^{\circ}\text{C}$) and oils and oil-based mono and hybrid nanofluids for medium temperature ($100\text{ }^{\circ}\text{C}$ to $250\text{ }^{\circ}\text{C}$). Effects of various modelling assumptions and heat flux distribution of heater on steady-state and transient performances are studied as well.

For numerical investigation, the different water-based binary and ternary hybrid nanofluids with $\text{Al}_2\text{O}_3+\text{Ag}$, $\text{Al}_2\text{O}_3+\text{Cu}$, $\text{Al}_2\text{O}_3+\text{TiO}_2$, $\text{Al}_2\text{O}_3+\text{CNT}$, and $\text{Al}_2\text{O}_3+\text{Graphene}$ and ternary hybrid nanofluids with $\text{Al}_2\text{O}_3+\text{Cu}+\text{CNT}$, $\text{Al}_2\text{O}_3+\text{Cu}+\text{Graphene}$,

$\text{Al}_2\text{O}_3+\text{CNT}+\text{Graphene}$, $\text{Cu}+\text{CNT}+\text{Graphene}$, for 1% volume concentration of nanoparticles, are selected. Also, the different thermal oils, viz. Therminol VPI, Paratherm CR, Dowtherm A, and Dowtherm Q are selected as the base fluids for further investigations. The investigations include the effect of the shape of nanoparticles, geometrical parameters like diameter, height, loop aspect ratio (height to width), loop inclination, nanoparticle shapes, and power input on the energetic and exergetic performance, viz. mass flow rate, effectiveness, and total entropy generation rate of a single-phase natural circulation loop. The results reveal that (a) the energetic and exergetic performance for the binary and ternary nanofluid is better than the respective base fluids. Moreover, ternary nanofluid shows better performance than binary nanofluids, (b) Paratherm CR shows a better performance among all thermal oils, (c) the shape of nanoparticles significantly affect the performance by influencing the mass flow rate, (d) the time required to attain a steady state is reduced with nanofluids, which is beneficial for a system, (e) the mass flow rate and the time required to achieve the steady state increase with tube diameter and height, (f) the effectiveness and entropy generation rate increase with decreasing loop diameter and height, (g) for a low input power the flow stabilizes at an early instant, and the steady state mass flow rate increases, (h) effectiveness decreases and entropy generation increases with increasing heater power, and (i) with the increasing loop aspect ratio the steady-state heat transfer effectiveness decreases, and the total entropy generation rate and the mass flow rate increases at an input power. The optimum value of the height to width ratio can be different for different types of fluids.

A detailed numerical investigation on the effect of different assumptions related to Boussinesq approximation, thermophysical properties, bend loss, heat loss, axial conduction of fluid, and wall conduction on the transient and steady-state characteristics has also been carried out. The effect of assumptions on the above-explained performance

parameters for different working fluids, viz. water, brines, and hybrid nanofluids, and the effect of different heat flux distributions, like the uniform, linear, non-linear, sinusoidal, and Gaussian, applied to heater have been explored. The results reveal that using the Boussinesq approximation, the error in the performance parameter is higher for EG and PG brine fluids, which restricts its use for all the fluids. The simulations with non-Boussinesq with temperature-dependent properties, including wall and fluid conduction, bend loss and heat loss, provide the closest agreement with the experiment for steady and transient behavior of a single-phase natural circulation loop.

Finally, experimental investigations are performed to evaluate the transient and steady-state performance of the selected single-phase natural circulation loop using mono and hybrid nanofluids that are based on water, Therminol VP1 and Soyabean oil. The nanoparticles and their combinations, viz. Al_2O_3 , $\text{Al}_2\text{O}_3+\text{CuO}$, $\text{Al}_2\text{O}_3+\text{SiC}$, and $\text{Al}_2\text{O}_3+\text{MWCNT}$ are selected for a volumetric concentration up to 0.1%. Here, the effect of input power, loop inclination (counter-clockwise and clockwise), and coolant inlet temperature on the performance parameters have been investigated. The result reveals (a) Therminol VP1 shows better performance than the Soyabean oil, (b) $\text{Al}_2\text{O}_3+\text{CNT}$ nanoparticles-based hybrid nanofluid shows the best performance among other hybrid nanofluids, (c) the increasing coolant inlet temperature enhances the mass flow rate and total entropy generation rate and reduces the effectiveness, (d) the decreasing loop inclination reduces the mass flow rate, whereas it increases the effectiveness and total entropy generation rate.

